

## Ca<sup>2+</sup> sparks involving multiple Ca<sup>2+</sup> release sites along Z-lines in rat heart cells

Ian Parker\*, Wei-Jin Zang and W. Gil Wier†

*Department of Physiology, University of Maryland, School of Medicine, Baltimore, MD 21201 and \*Laboratory of Cellular and Molecular Neurobiology, Department of Psychobiology, University of California, Irvine, CA 92717, USA*

1. High spatial resolution confocal imaging was used to investigate the fundamental nature of 'Ca<sup>2+</sup> sparks' in rat cardiac myocytes loaded with the fluorescent calcium indicator, fluo-3.
2. The sites at which calcium sparks occurred (Ca<sup>2+</sup> release sites) were packed closely and irregularly in transverse planes along Z-lines (mean spacing between sites of 0.76  $\mu\text{m}$ ). In contrast, sites were spaced more regularly in the longitudinal direction, at intervals of 1.8  $\mu\text{m}$  (i.e. the sarcomere length).
3. Diffusion of released Ca<sup>2+</sup> was slower transversely (apparent diffusion coefficient,  $D$ , 7.9  $\mu\text{m}^2 \text{s}^{-1}$ ) than longitudinally ( $D$ , 17.1  $\mu\text{m}^2 \text{s}^{-1}$ ).
4. Frequently, discrete sites several hundred nanometres apart transversely activated in near synchrony. The probability of transverse synchronous activity fell to low levels (< 20%) at sites separated by more than 1.0  $\mu\text{m}$ . Synchronous activation was not observed between sites on different Z-lines (i.e. separated longitudinally by 1.8  $\mu\text{m}$ ).
5. High temporal resolution confocal microscopy (stationary spot) revealed Ca<sup>2+</sup> sparks with 'stepped' rises, consistent with multiple sites of origin.
6. We conclude that the Ca<sup>2+</sup> spark as originally described is usually not an 'elementary' event, in the sense of being indivisible, but is often comprised of yet smaller, triggered units of Ca<sup>2+</sup> release.

Confocal fluorescence microscopy of cardiac myocytes loaded with Ca<sup>2+</sup> indicator has revealed that Ca<sup>2+</sup> liberation from the sarcoplasmic reticulum (SR) produces spatially localized [Ca<sup>2+</sup>]<sub>i</sub> transients or Ca<sup>2+</sup> 'sparks' (Cheng, Lederer & Cannell, 1993; see also Niggli & Lipp, 1992). Sparks occur spontaneously in resting cells, and can also be evoked by Ca<sup>2+</sup> influx through L-type plasma membrane Ca<sup>2+</sup> channels during cellular depolarization (López-López, Shacklock, Balke & Wier, 1994, 1995; Cannell, Cheng & Lederer, 1995). In line-scan confocal images oriented along the long axis of ventricular cells, sparks are seen to arise at sites spaced regularly at 1.8  $\mu\text{m}$  intervals corresponding to transverse tubules (t-tubules) at Z-lines (Shacklock, Wier & Balke, 1995). Each site appears to act as an autonomous functional unit generating asynchronous sparks. Estimates of the amount of Ca<sup>2+</sup> liberated during a spark led to the proposal (Cheng *et al.* 1993) that each unit is composed of only a single functional ryanodine receptor channel (RyR), although the alternative possibility, that sparks arise from more than one channel, could not be eliminated (Cheng *et al.* 1993). The concept that the Ca<sup>2+</sup> spark represents an elementary unit

of Ca<sup>2+</sup> release during excitation–contraction (E–C) coupling, triggered independently by Ca<sup>2+</sup> influx through L-type Ca<sup>2+</sup> channels (López-López *et al.* 1994, 1995; Cannell *et al.* 1995), is central in the 'local control' theory of cardiac E–C coupling (Stern, 1992; Wier, Egan, López-López & Balke, 1994; for review, see Bootman & Berridge, 1995). This concept helps to account for the graded control of Ca<sup>2+</sup> release with depolarization, despite the inherently regenerative nature of Ca<sup>2+</sup>-induced Ca<sup>2+</sup> release (CICR) from the SR.

This notion of elementary Ca<sup>2+</sup> release events applies also to the other major cellular Ca<sup>2+</sup> signalling pathway, which involves inositol trisphosphate receptors (InsP<sub>3</sub>Rs). In that pathway also, spatially localized transient signals (Ca<sup>2+</sup> 'puffs') closely resembling Ca<sup>2+</sup> sparks are seen (Yao, Choi & Parker, 1995; Bootman & Berridge, 1995). However, the puff is not the elementary unit of InsP<sub>3</sub>-mediated Ca<sup>2+</sup> release, since yet smaller transients (Ca<sup>2+</sup> 'blips') (Parker & Yao, 1996) have recently been resolved. The puff must therefore involve Ca<sup>2+</sup> release through multiple channels. Similarly, it has been proposed recently that Ca<sup>2+</sup> release in

† To whom correspondence should be addressed.



the heart may involve unresolved unitary events ( $\text{Ca}^{2+}$  quarks) much smaller than the spark (Lipp & Niggli, 1996). Using high temporal resolution stationary point confocal microscopy, we have observed in rat ventricular cells small units of  $\text{Ca}^{2+}$  release (compared with sparks), which we termed 'subsparks' (Parker & Wier, 1996). Our aim here was to use confocal imaging to study spontaneous  $\text{Ca}^{2+}$  sparks in rat ventricular myocytes to determine whether the spark could be dissected into smaller, discrete, spatially and temporally resolved release events. To this end we constructed a 'home-made' confocal microscope utilizing a high-efficiency detector and simplified optical path, which provided a spatial resolution ( $\sim 0.3 \mu\text{m}$ ) in line-scan mode better than our BioRad MRC 600 system, and a sub-millisecond temporal resolution in stationary point mode. The major finding is that sparks generally involve  $\text{Ca}^{2+}$

release from two or more sites, which activate within a few milliseconds of each other, and which are packed closely together at a Z-line.

## METHODS

### Preparation of cells

Two-month-old Sprague-Dawley rats (200–300 g) were anaesthetized with sodium pentobarbitone ( $17 \text{ mg kg}^{-1}$  injected i.p.). The hearts were removed from the animals via mid-line thoracotomy, and single ventricular cells were obtained by an enzymatic technique described in detail previously (López-López *et al.* 1995). The myocytes were loaded with the fluorescent  $\text{Ca}^{2+}$  indicator fluo-3 by incubation for  $> 30 \text{ min}$  with  $5 \mu\text{M}$  fluo-3 AM (Molecular Probes, Inc). Cells were imaged through a Nikon Diaphot inverted microscope with a  $\times 60$  plan-apo oil-immersion objective (NA, 1.4). Recordings of  $\text{Ca}^{2+}$  sparks were made in normal Tyrode solution

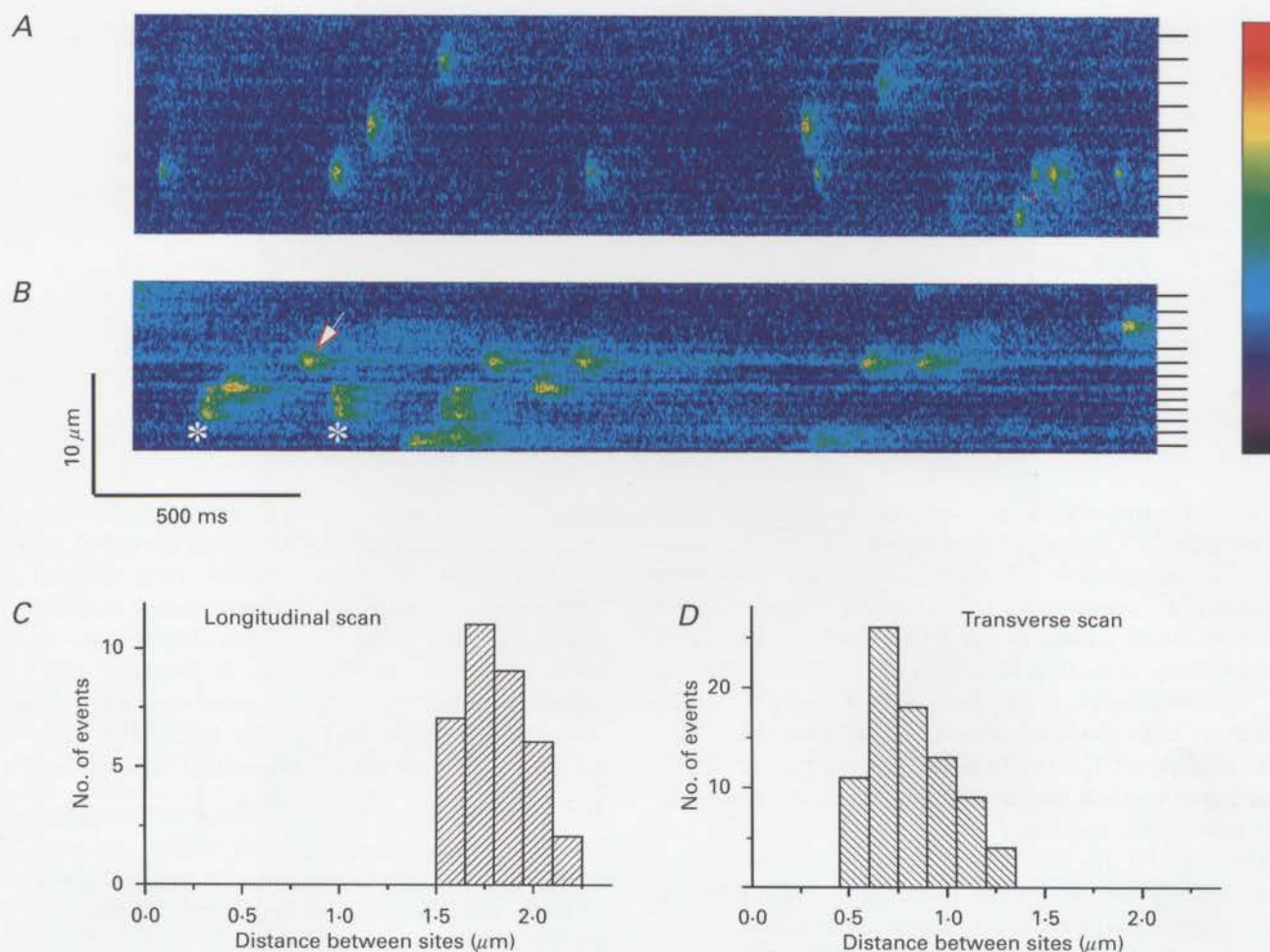


Figure 1. Calcium sparks visualized by line-scan imaging longitudinally and transversely across fluo-3-loaded rat ventricular myocytes

A and B, line-scan images showing distance along the scan lines depicted vertically, and successive scan lines at 3 ms intervals stacked from left to right; increasing  $\text{Ca}^{2+}$ -dependent fluorescence is coded as indicated by the colour bar. Lines at the right mark positions of all sites showing sparks throughout 25 s recording periods. The image in A was obtained with the scan line oriented along the long axis of a cell, and that in B by scanning transversely across a different cell. In B, asterisks indicate  $\text{Ca}^{2+}$  sparks arising at multiple sites. The arrow indicates a  $\text{Ca}^{2+}$  spark arising at only one site. C and D, distributions of minimal spacings between spark sites measured from 6 longitudinal and 28 transverse line-scan images, respectively.

(composition, mM: NaCl, 140; dextrose, 10; Hepes, 10; KCl, 4.0;  $\text{MgCl}_2$ , 1;  $\text{CaCl}_2$ , 1; pH adjusted to 7.3–7.4 with NaOH) at room temperature (22 °C), with  $[\text{Ca}^{2+}]_0$  between 0.5 and 2 mM.

### Confocal microscopy

Line-scan images were obtained using a home-made confocal scanner, which provided a spatial resolution superior to our BioRad MRC 600 system and allowed continuous image recording for up to 25 s. The 488 nm beam from a 100 mW argon ion laser (Omnichrome, Chino, CA, USA) was attenuated 10- to 100-fold and expanded to overfill the objective back aperture. A galvanometer-driven mirror (Cambridge Technology, Watertown, MA, USA) repeatedly scanned the laser spot along a line about 20  $\mu\text{m}$  long every 3 ms. Cells were rotated to align the scan line along either the long axis of the cell or transversely (parallel to the striations). Fluorescence emission was descanned by the same mirror, long-pass filtered at  $\lambda > 515$  nm and, after passing through a confocal aperture transmitting only the central peak of the Airy disc, was focused onto an avalanche diode photon counting module (SPCM-AQ-121; EG & G Canada Ltd, Dumberry, Vaudreuil, Quebec, Canada). The point-spread function, measured using 0.1  $\mu\text{m}$  fluorescent beads, was 0.31  $\mu\text{m}$  laterally (full width at half-

maximum after subtracting bead diameter) and 0.41  $\mu\text{m}$  axially. Photon counts were integrated by a 30 kHz low-pass filter, combined with sync pulses marking the mirror fly-back, and sampled at 10  $\mu\text{s}$  intervals (pixel size, 0.1  $\mu\text{m}$ ) for gap-free storage on computer disk using the pCLAMP software package (Axon Instruments). Finally, line-scan images were constructed by custom routines written in the IDL programming language (Research Systems, Inc., Boulder, CO, USA). Stationary point confocal microscopy (Fig. 4C) was performed with the mirror stationary, and digitizing the fluorescence at 2 kHz. Fluorescence signals are expressed as fractional increases above resting level ( $\Delta F/F_0$ ).

## RESULTS

### Sparks visualized in longitudinal and transverse scans

Images of resting rat cardiac myocytes obtained by scanning the confocal spot along the length of the cell showed spontaneous  $\text{Ca}^{2+}$  sparks (Fig. 1A and C), which originated at apparent point sources ( $< 400$  nm diameter) spaced at

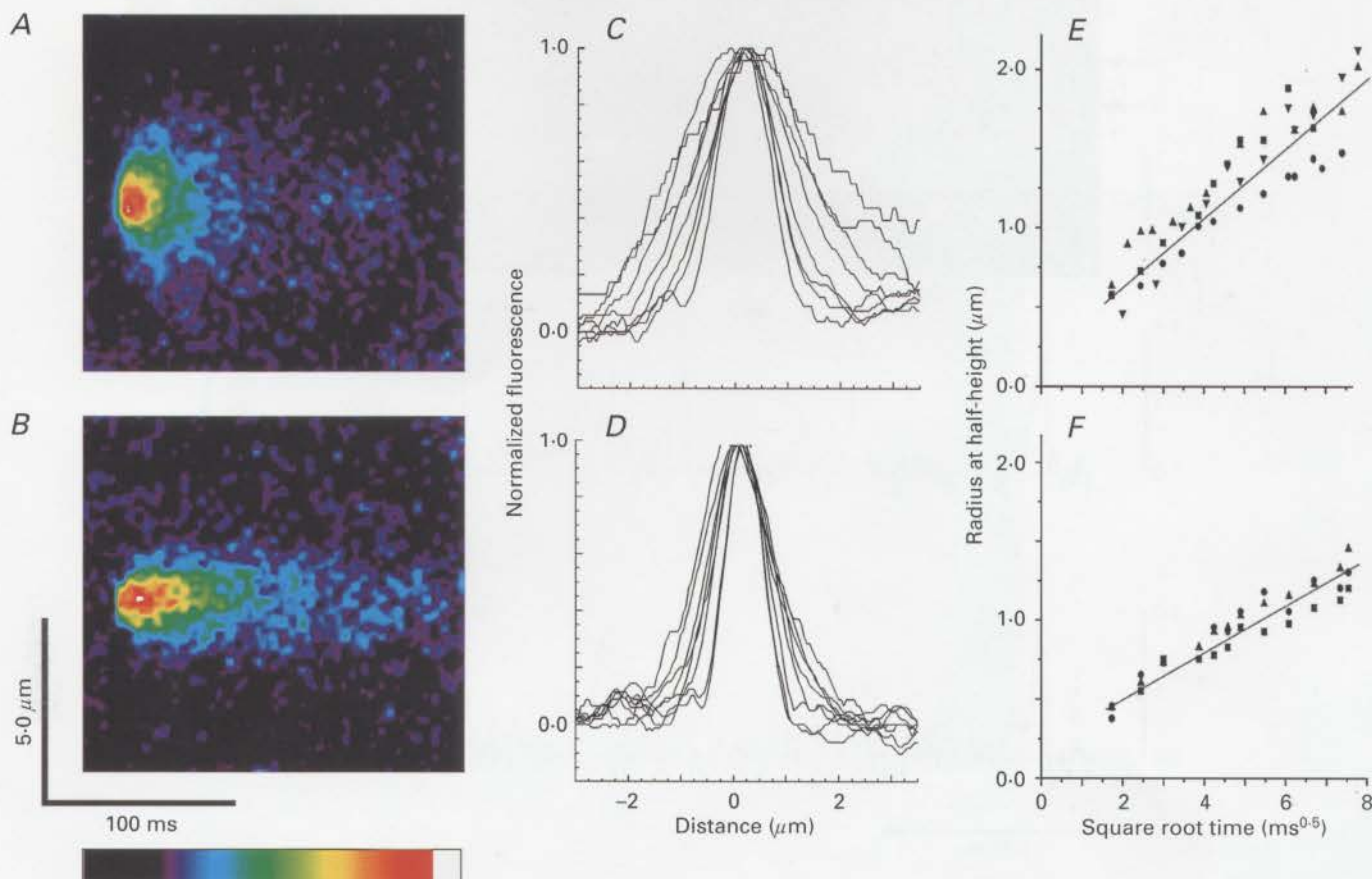


Figure 2. Longitudinal and transverse diffusion of  $\text{Ca}^{2+}$ -activated fluorescence during  $\text{Ca}^{2+}$  sparks

Line-scan images showing averages of 11 events at a single site scanned longitudinally (A) and 4 events at a different site scanned transversely (B), constructed by aligning the rising phases of individual events and displayed after subtraction of background fluorescence. C and D, intensity profiles along the scan lines at 6, 9, 12, 18, 27, 36, 48 and 78 ms after the beginning of the signals, normalized to the same maximal intensities. Profiles were averaged over 2, 3 or 5 adjacent scan lines and smoothed by a running average over 5 pixels (0.5  $\mu\text{m}$ ). The width of the profiles increases progressively with time. E and F, measurements of the radial spread of the fluorescence signal at half-amplitude obtained from profiles like those in C and D, plotted against the square root of time, with  $t = 0$  taken as 3 ms prior to the first detectable rise of  $\text{Ca}^{2+}$ .



regular intervals of about  $1.8\ \mu\text{m}$  (bars in Fig. 1A) consistent with  $\text{Ca}^{2+}$  release from discrete sites associated with the sarcomeric structure of the cell. Previous work has shown that these sites are closely associated with transverse (t)-tubules and are thus at Z-lines (Shacklock *et al.* 1995). These sites were further marked by a small elevation in background fluorescence (faint horizontal lines in Fig. 1A), possibly resulting from compartmentalized or otherwise immobilized  $\text{Ca}^{2+}$ -insensitive indicator (Tsugorka, Rios & Blatter, 1995). At each site, a  $\text{Ca}^{2+}$  spark occurred autonomously at least once during the 25 s period of this recording. Except during propagating  $\text{Ca}^{2+}$  waves (Takamatsu & Wier, 1990), we never observed in such longitudinal scans instances where a spark at one site triggered a localized spark at an adjacent site ( $> 100$  records examined).

In contrast, transverse line-scan images (scanned at 90 deg to the long axis of the cell) showed sparks with very different characteristics. Spacings between spark sites

(Fig. 1D) were smaller and less regular than in longitudinal scans (compare bars in Fig. 1A and B), and correlated with a closer and more heterogeneously distributed pattern of background fluorescence. The sparks were also more variable in appearance, with some showing a more restricted spatial spread than in longitudinal scans (arrow), while others (asterisks) presented a 'blunt' appearance and appeared to arise through near-synchronous release of  $\text{Ca}^{2+}$  at several discrete, adjacent sites.

#### Longitudinal and transverse diffusion of $\text{Ca}^{2+}$

The restricted spread of the  $\text{Ca}^{2+}$  signal in transverse scans of sparks that appeared to arise from single sites suggested that diffusion in myocytes is more restricted radially than longitudinally. Quantitative analysis was performed on averaged images from multiple events at single sites scanned longitudinally (Fig. 2A) and transversely (Fig. 2B). Both sparks showed a characteristic 'comet tail' appearance and, consistent with a diffusional process, the spatial profiles of

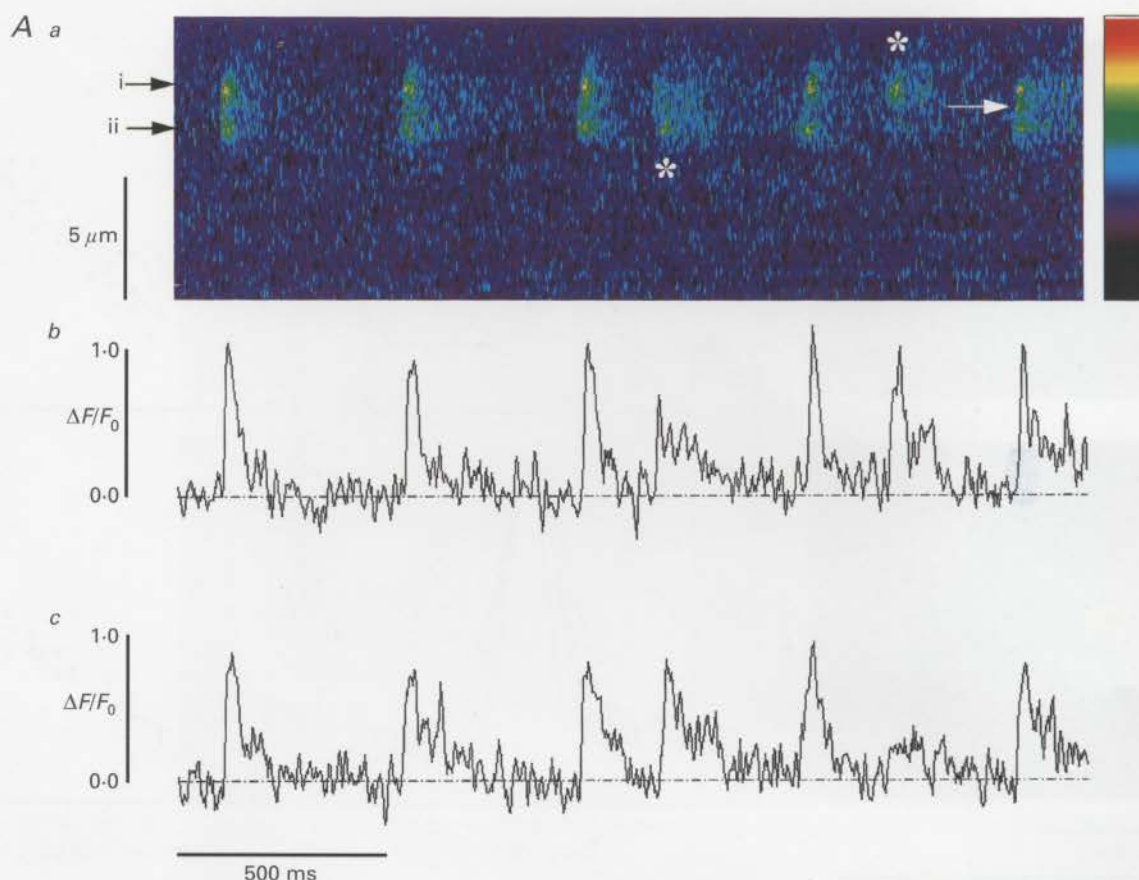


Figure 3. Analysis of coupled  $\text{Ca}^{2+}$  release from discrete transverse sites  $1.4\ \mu\text{m}$  apart

*Aa* (above), transverse line-scan image (background subtracted and smoothed by averaging over 5 pixels along the scan line) showing spontaneous events occurring synchronously at two sites, and examples of events involving only single sites (\*). *b* and *c*, changes in fluorescence monitored at the two sites indicated by *i* and *ii* in *Aa*. Traces are an average over 5 pixels (500 nm) and are smoothed by a running average over 3 lines (9 ms). *Ba* (on facing page), averaged, background-subtracted image formed from 34 events involving synchronous signals at both the sites marked in *Aa*. Traces *b* and *c* show profiles of fluorescence intensity (3 line average, smoothed over 5 pixels) along the scan line at times marked by the arrows in *Ba*. *d-g*, similar images and line profiles for averages of 5 (*d*) and 4 (*f*) events involving release at one or other of the individual sites.

longitudinally and transversely scanned sparks followed roughly Gaussian distributions (Fig. 2*C* and *D*) whose widths increased as the square root of time (Fig. 2*E* and *F*). The fluorescence signal spread more slowly in transverse scans, and calculation (Yao *et al.* 1995) of the apparent diffusion coefficient,  $D$ , from the slopes of the lines in Fig. 2*E* and *F* (where  $D = (\text{slope})/(-4 \ln 2)$ ) yielded values of  $17.1 \mu\text{m}^2 \text{s}^{-1}$  longitudinally and  $7.9 \mu\text{m}^2 \text{s}^{-1}$  transversely. Since these values are derived from the spread of the fluorescence signal

they reflect diffusion of  $\text{Ca}^{2+}$ -bound indicator rather than diffusion of free  $\text{Ca}^{2+}$  *per se*, which is likely to be further slowed by binding to immobile buffer. Nevertheless, it is clear that diffusion within cardiac myocytes is anisotropic.

### Synchronous $\text{Ca}^{2+}$ release at multiple sites

Despite the more restricted radial diffusion of  $\text{Ca}^{2+}$ , transverse scans revealed that many sparks involved  $\text{Ca}^{2+}$  signals arising at two or more discrete sites (e.g. Fig. 1*B*),

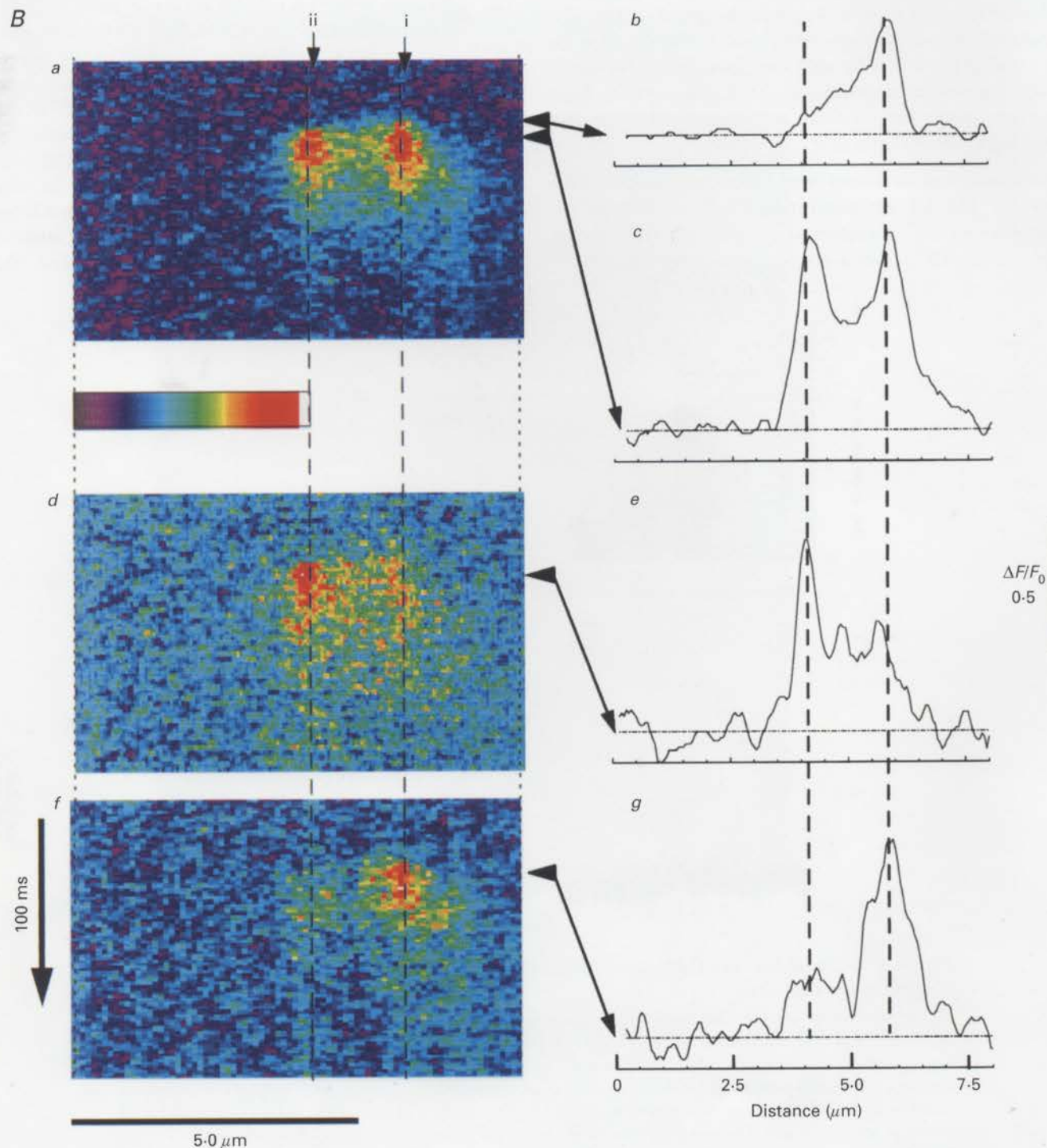


Figure 3*B*. For legend see facing page.



probably because a close radial packing of release sites at Z-lines allows  $\text{Ca}^{2+}$  spreading from one site to induce  $\text{Ca}^{2+}$  release ( $\text{Ca}^{2+}$ -induced  $\text{Ca}^{2+}$  release, or CICR) at closely adjacent sites. The spatial resolution of the confocal microscope was sufficient to allow events to be reliably categorized as involving single or multiples sites at spacings down to about 600 nm. However, more detailed study of the coupling between sites was difficult with such closely adjacent signals. We therefore selected a record for further analysis in which coupled activity was seen between two well-resolved sites (i and ii) 1.4  $\mu\text{m}$  apart (Fig. 3A). The probability of paired events (80%) was unusually high for this spacing (cf. Fig. 4B), and may have arisen because a poorly resolved intermediate site (Fig. 3A, arrow), lying above or below the confocal section, served to couple triggering at the outlying sites.

The occurrence of occasional events involving just one or the other site (Fig. 3A, asterisks) indicates that double sparks arose through  $\text{Ca}^{2+}$  liberation at two discrete sites, rather than because  $\text{Ca}^{2+}$  from a single source was detected by

separate regions of high indicator concentration, and averaged images from multiple double (Fig. 3Ba–c) and single (Fig. 3Bd–g) events at these sites illustrate the clear separation between  $\text{Ca}^{2+}$  signals at the two sites. Further, profiles of  $\text{Ca}^{2+}$ -dependent fluorescence along the scan line during apparent single-site events (Fig. 3Be and g) showed small elevations at the second sites, which may have arisen through activation of a small, non-regenerative  $\text{Ca}^{2+}$  liberation.

$\text{Ca}^{2+}$  liberation began on average earlier at site i (Fig. 3Ba and b), suggesting that this was the more active site which functioned as a pacemaker, though variation in relative latencies (Fig. 4A) further indicates that the two sites do not reflect a single source of  $\text{Ca}^{2+}$ . In some instances  $\text{Ca}^{2+}$  at sites i and ii rose almost simultaneously, possibly because  $\text{Ca}^{2+}$  from a poorly resolved intermediate site triggered near-simultaneous activation of the outlying sites. In most remaining events, release at site i began about 6 ms before site ii, though the inverse case involving similar latencies was observed in a few instances (cross-hatched bars). This

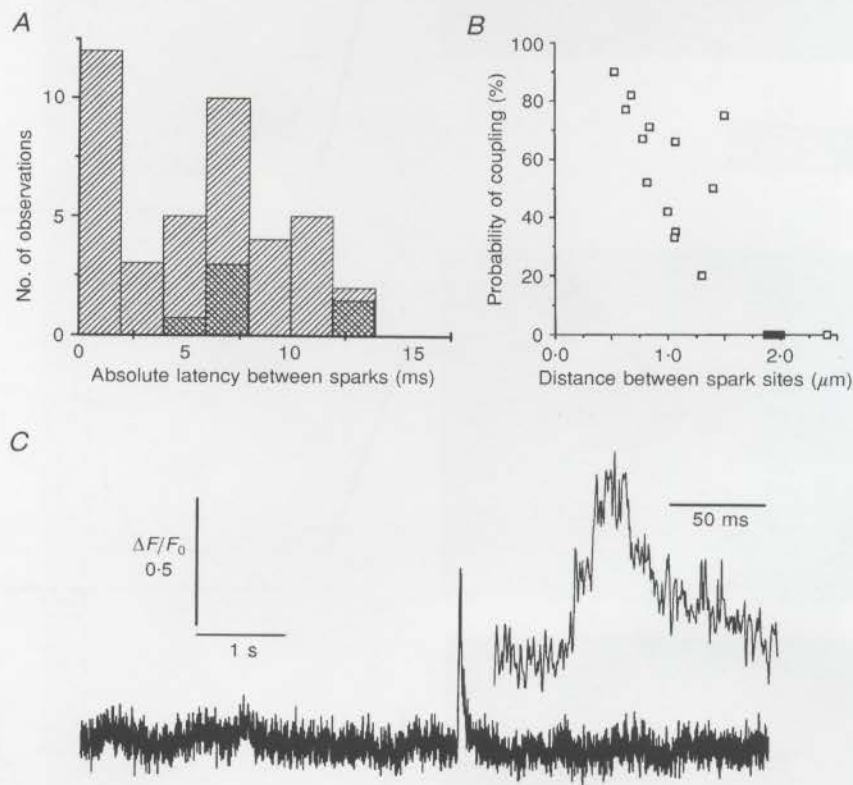


**Figure 4.** Latencies between  $\text{Ca}^{2+}$  release at paired sites and probability of coupling as a function of distance between sites

A, distribution of absolute latencies between rise in fluorescence at the 2 sites illustrated in Fig. 3. ▨, instances ( $n = 6$ ) when site ii activated first; ▩, instances when site i was first ( $n = 29$ ) or when there was no detectable latency ( $n = 12$ ). B, probability of coupled activation between pairs of adjacent release sites as a function of separation between the sites. Points represent the percentage of total events (sparks at either or both sites) involving near-synchronous ( $< 15$  ms) activation of both sites. Data were derived from events at 18 paired sites. Open symbols are from transverse scans, filled symbols from longitudinal scans. C, high temporal resolution stationary-point confocal recording of a  $\text{Ca}^{2+}$  spark. The main (lower) trace is a continuous recording showing a single spark. The inset at a higher sweep speed shows the 'stepped' rising phase of this spark, with a delay between first rise and second rise of 9 ms.



lag of about 6 ms over a distance of  $1.4 \mu\text{m}$  corresponds to a velocity of roughly  $230 \mu\text{m s}^{-1}$ , about twice as fast as reported for  $\text{Ca}^{2+}$  wave propagation (Takamatsu & Wier, 1990; Cheng, Lederer, Lederer & Cannell, 1996).

The latency between  $\text{Ca}^{2+}$  signals provides a powerful argument for release being triggered at spatially distinct sites. However, the brief times involved are barely resolved by the line-scan technique, and then only in favourable cases like that in Fig. 3, with widely separated sites. To resolve better the 'steps' in the rise of  $\text{Ca}^{2+}$  sparks that would be expected from short latency coupling between release sites, we recorded continuously (2 kHz sampling rate) from a stationary confocal spot. In this recording mode, steps were sometimes detected (Fig. 4C), probably because the confocal spot volume ( $\sim 10^{-15}$  l) lay between two sites, one of which activated earlier (9 ms; Fig. 4C, inset) than the other.

### Probability of coupling between sites

Well-resolved records were obtained in a total of twenty-one transverse line-scan images (total of 633 events in 17 cells). Of these events, 32% apparently involved release from only a single site, 59% from two sites, 9% from three or more sites. Thus, a majority of events involved multiple sites. Moreover, the values above probably underestimate both the proportion of events involving release at more than one site and the average number of sites which activate synchronously, since separate sites displaced in the  $z$ -axis or separated laterally by  $< 600$  nm would not have been resolved. The probability of synchronous release at adjacent sites declined steeply with increasing separation between sites (Fig. 4B), falling to zero by the sarcomere spacing at  $1.8 \mu\text{m}$ . Previous studies of  $\text{Ca}^{2+}$  sparks (Cheng *et al.* 1993; Shacklock *et al.* 1995) have generally utilized longitudinal scanning with a spatial resolution ( $0.5$ – $0.8 \mu\text{m}$  lateral,  $1$ – $2 \mu\text{m}$  axial, pixel size  $0.27 \mu\text{m}$ ) less good than achieved here (see Methods and Fig. 1), so that resolution of discrete events separated by less than  $1.0 \mu\text{m}$  would have been more problematic.

## DISCUSSION

The major results are that  $\text{Ca}^{2+}$  released from the SR produces sparks at discrete sites, which are packed at high density transversely across the cell as compared with their longitudinal spacing at the sarcomere length, and that two or more such transverse sites often generate sparks in near synchrony. These phenomena were not observed in previous studies of  $\text{Ca}^{2+}$  sparks (Cheng *et al.* 1993; Shacklock *et al.* 1995), in part because recordings were generally made utilizing longitudinal scanning. We discuss below the fact that longitudinal scanning is intrinsically less capable of resolving nearly synchronous  $\text{Ca}^{2+}$  release at sites spaced closely in the transverse direction. In addition, some of the previous studies have cited a spatial resolution ( $0.5$ – $0.8 \mu\text{m}$  lateral,  $1$ – $2 \mu\text{m}$  axial, nominal pixel size  $0.27 \mu\text{m}$ ) less good than achieved here. Most importantly, however, longitudinal scanning of sites having nearly synchronous activity with

neighbouring sites at the same Z-line would produce only steps in the rising phase of the line-scan images of the  $\text{Ca}^{2+}$  sparks, reflecting the delay between activation of the sites and time for  $\text{Ca}^{2+}$  to diffuse. This delay is usually short, however, compared with the typical time per scan line ( $2$ – $4$  ms) and would therefore be nearly impossible to resolve. In summary, multiple sites of release at a given Z-line can be readily resolved in the spatial dimension with high-resolution transverse scanning, but not in the temporal domain by longitudinal scanning. Thus, although  $\text{Ca}^{2+}$  sparks were originally proposed to arise from  $\text{Ca}^{2+}$  flux through single RyRs (Cheng, *et al.* 1993), the finding that a majority of  $\text{Ca}^{2+}$  release events involve two or more sites hundreds of nanometres apart indicates that multiple RyRs or multiple clusters of RyRs must be involved.

In our transverse line-scan recordings, roughly two-thirds of all events involved near-simultaneous release at two or (rarely) three discrete sites. This result is unlikely to have arisen as a result of  $\text{Ca}^{2+}$  overload, as the phenomenon persists in cells bathed in low ( $0.5$  mM) extracellular  $[\text{Ca}^{2+}]$ , and cells showed low frequencies of spontaneous  $\text{Ca}^{2+}$  waves ( $0.5$  mM  $\text{Ca}_0^{2+}$ ,  $0.6$  waves  $\text{min}^{-1}$ ;  $1.0$  mM  $\text{Ca}_0^{2+}$ ,  $1.0$  waves  $\text{min}^{-1}$ ;  $2.0$  mM  $\text{Ca}_0^{2+}$ ,  $2.8$  waves  $\text{min}^{-1}$ ). Also, it is likely that the mean number of sites involved in each event is higher than suggested by the above value, since adjacent sites above or below one another, or displaced laterally by less than about  $0.6 \mu\text{m}$ , would not be separately resolved. It remains to be determined, however, what factors limit the extent of synchronous activation to just a few neighbouring sites, rather than allowing propagation of a  $\text{Ca}^{2+}$  wave at release sites across entire Z-discs.

$\text{Ca}^{2+}$  release sites were present at regular spacings of  $1.8 \mu\text{m}$  longitudinally, and at more irregular spacing with a mean of about  $0.76 \mu\text{m}$  transversely, corresponding to an average of about one site per femtolitre ( $10^{-15}$ ) of cell volume. Further, sites of spark initiation matched closely to regions of elevated resting fluo-3 fluorescence in both longitudinal and transverse scans (Fig. 1A and B). Although the reason for these variations in resting fluorescence is not known,  $x$ - $y$  confocal images of quiescent, fluo-3 loaded cells provide a useful 'map' of the distribution of potential release sites (data not shown). There is little doubt that sparks arise longitudinally at the position of the t-tubules (Shacklock *et al.* 1995). The lateral distribution of spark sites (Fig. 1B) also roughly matches to the 'beaded' appearance of t-tubules along the Z-lines, which may arise as the tubules snake in and out of the plane of the confocal section. In agreement with these studies at the light microscopic level, electron micrographs indicate that RyRs are organized in clusters (Ferguson, Schwartz & Franzini-Armstrong, 1984) at the terminal SR-transverse tubule junction. Longitudinally, junctions are separated by about  $1.8 \mu\text{m}$  but the transverse spacings are substantially smaller (Amsellem, Delorme, Souchier & Ojeda, 1995).

One major question still remaining to be answered concerns whether the  $\text{Ca}^{2+}$  signal at a single site (as we resolve it)



involves opening of a single RyR, or the concerted activation of a tight cluster of several RyRs. On the one hand, our estimate of the density of release sites (1 per  $10^{-15}$  l) suggests that a single channel per site, passing a  $\text{Ca}^{2+}$  current of 3 pA for 5 ms ( $1.5 \times 10^{-14}$  C or  $7.75 \times 10^{-20}$  mol of  $\text{Ca}^{2+}$ ) would be sufficient to account for the entire amount of  $\text{Ca}^{2+}$  released during an action potential ( $\sim 1 \times 10^{-4}$  mol  $\text{l}^{-1}$  of accessible cell volume or  $1 \times 10^{-19}$  mol  $\text{fl}^{-1}$ ; Sipido & Wier, 1991). On the other hand, electron microscopic studies indicate that RyRs are organized into clusters some tens of nanometres in size, and it seems improbable that  $\text{Ca}^{2+}$  released through one channel would fail to activate other channels within the cluster while still triggering release at much more distant sites as much as  $1 \mu\text{m}$  away.

A possible reconciliatory explanation of the paradox raised above would be that, in fact, several RyRs within one or more clusters at a Z-line are activated in a  $\text{Ca}^{2+}$  spark, but each RyR passes  $\text{Ca}^{2+}$  fluxes smaller than described above (3 pA for 5 ms). On this basis,  $\text{Ca}^{2+}$  release at one of the multiple foci observed in the present study could not be identical to the  $\text{Ca}^{2+}$  'quark', which is a putative, very small change in  $[\text{Ca}^{2+}]_i$  that has been proposed to result from the gating of a single RyR (Lipp & Niggli, 1996). Rather, in our favoured explanation, each focus of release might consist of several, as yet unresolved,  $\text{Ca}^{2+}$  quarks. The alternative (and unlikely) possibility is that each focus of release along a Z-line involves the opening of only one channel (i.e. the 'quark') within a cluster of otherwise 'silent' or unavailable RyRs, whilst still permitting the activation of an RyR within a neighbouring cluster.

In conclusion, therefore, it appears that a  $\text{Ca}^{2+}$  spark is not the elementary unit of  $\text{Ca}^{2+}$  liberation, but is often composed of yet smaller, triggered units of  $\text{Ca}^{2+}$  release occurring at discrete sites spaced at distances of several hundred nanometres transversely across the cell, at the Z-discs. Preliminary results (I. Parker, C. W. Balke, W.-J. Zang & W. G. Wier, unpublished observations) indicate that a similar coupling of elemental release events occurs also during  $\text{Ca}^{2+}$  release evoked by depolarization. This would be expected if  $\text{Ca}^{2+}$  release triggered at one site by  $\text{Ca}^{2+}$  entry through an immediately adjacent L-type  $\text{Ca}^{2+}$  channel served, in turn, to trigger neighbouring release sites, and the multiplicative effect of coupling between sites may serve to enhance the overall 'gain' of E-C coupling (Stern, 1992; Wier *et al.* 1994).

AMSELLEM, J. A., DELORME, R., SOUCHIER, C. & OJEDA, C. (1995). Transverse-axial tubular system in guinea pig ventricular cardiomyocyte: 3D reconstruction, quantification and its possible role in  $\text{K}^+$  accumulation-depletion phenomenon in single cells. *Biology of the Cell* **85**, 43–54.

BOOTMAN, M. D. & BERRIDGE, M. J. (1995). The elemental principles of calcium signals. *Cell* **83**, 675–678.

CANNELL, M. B., CHENG, H. & LEDERER, W. J. (1995). The control of calcium release in heart muscle. *Science* **268**, 1045–1049.

CHENG, H., LEDERER, W. J. & CANNELL, M. B. (1993). Calcium sparks: Elementary events underlying excitation-contraction coupling in heart muscle. *Science* **262**, 740–744.

CHENG, H., LEDERER, M. R., LEDERER, W. J., & CANNELL, M. B. (1996). Calcium sparks and  $[\text{Ca}^{2+}]_i$  waves in cardiac myocytes. *American Journal of Physiology* **270**, C148–159.

FERGUSON, D. G., SCHWARTZ, H. W. III & FRANZINI-ARMSTRONG, C. (1984). Subunit structure of junctional feet in triads of skeletal muscle: a freeze-drying, rotary-shadowing study. *Journal of Cell Biology* **99**, 1735–1742.

LIPP, P. & NIGGLI, E. (1996). Submicroscopic calcium signals as fundamental events of excitation-contraction coupling in guinea-pig cardiac myocytes. *Journal of Physiology* **492**, 31–38.

LÓPEZ-LÓPEZ, J. R., SHACKLOCK, P. S., BALKE, C. W. & WIER, W. G. (1994). Local, stochastic release of  $\text{Ca}^{2+}$  in voltage-clamped rat heart cells: visualization with confocal microscopy. *Journal of Physiology* **480**, 21–29.

LÓPEZ-LÓPEZ, J. R., SHACKLOCK, P. S., BALKE, C. W. & WIER, W. G. (1995). Local calcium transients triggered by single L-type calcium channel currents in cardiac cells. *Science* **268**, 1042–1045.

NIGGLI, E. & LIPP, P. (1992). Spatially restricted  $\text{Ca}^{2+}$ -release in cardiac myocytes revealed by confocal microscopy. *Pflügers Archiv* **420**, suppl. 1, R81.

PARKER, I. & WIER, W. G. (1996).  $\text{Ca}^{2+}$  sparks studied by stationary point confocal femtofluorimetry. *Journal of Molecular and Cellular Cardiology* **28**, A132.

PARKER, I. & YAO, Y. (1996).  $\text{Ca}^{2+}$  transients associated with openings of inositol trisphosphate-gated channels in *Xenopus* oocytes. *Journal of Physiology* **491**, 663–668.

SHACKLOCK, P. S., WIER, W. G. & BALKE, C. W. (1995). Local  $\text{Ca}^{2+}$  transients ( $\text{Ca}^{2+}$  sparks) originate at transverse tubules in rat heart cells. *Journal of Physiology* **487**, 601–608.

SIPIDO, K. R. & WIER, W. G. (1991). Flux of  $\text{Ca}^{2+}$  across the sarcoplasmic reticulum of guinea-pig cardiac cells during excitation-contraction coupling. *Journal of Physiology* **435**, 605–630.

STERN, M. D. (1992). Theory of excitation-contraction coupling in cardiac muscle. *Biophysical Journal* **63**, 497–517.

TAKAMATSU, T. & WIER, W. G. (1990). Calcium waves in mammalian heart: Quantification of origin, magnitude, waveform and velocity. *FASEB Journal* **4**, 1519–1525.

TSUGORKA, A., RIOS, E. & BLATTER, L. A. (1995). Imaging elementary events of calcium release in skeletal muscle cells. *Science* **269**, 1723–1726.

WIER, W. G., EGAN, T. M., LÓPEZ-LÓPEZ, J. R. & BALKE, C. W. (1994). Local control of excitation-contraction coupling in rat heart cells. *Journal of Physiology* **474**, 463–471.

YAO, Y., CHOI, J. & PARKER, I. (1995). Quantal puffs of intracellular  $\text{Ca}^{2+}$  evoked by inositol trisphosphate in *Xenopus* oocytes. *Journal of Physiology* **482**, 533–553.

### Acknowledgements

Financial support was provided by NIH grants to Ian Parker (GM48071) and W. Gil Wier (HLBI 29473 and HLBI 55280).

### Author's email address

W. G. Wier: gil@wgv.ab.umd.edu

Received 20 August 1996; accepted 23 September 1996.